UCSF
UC San Francisco Previously Published Works

Title

Multidimensional Analysis of Magnetic Resonance Imaging Predicts Early Impairment in Thoracic and Thoracolumbar Spinal Cord Injury

Permalink

https://escholarship.org/uc/item/8qk6d1m2

Journal

Journal of Neurotrauma, 33(10)

ISSN

0897-7151

Authors

Mabray, Marc C
Talbott, Jason F
Whetstone, William D
et al.

Publication Date

2016-05-15

DOI

10.1089/neu.2015.4093

Peer reviewed

eScholarship.org Powered by the California Digital Library
University of California

JOURNAL OF NEUROTRAUMA 33:954–962 (May 15, 2016)
© Mary Ann Liebert, Inc.
DOI: 10.1089/neu.2015.4093

Multidimensional Analysis of Magnetic Resonance Imaging Predicts Early Impairment in Thoracic and Thoracolumbar Spinal Cord Injury

Marc C. Mabray,[1] Jason F. Talbott,[1,5] William D. Whetstone,[2,5] Sanjay S. Dhall,[3,5] David B. Phillips,[3,5] Jonathan Z. Pan,[4,5] Geoffrey T. Manley,[3,5] Jacqueline C. Bresnahan,[3,5] Michael S. Beattie,[3,5] Jenny Haefeli,[3,5] and Adam R. Ferguson[3,5,6]

Abstract

Literature examining magnetic resonance imaging (MRI) in acute spinal cord injury (SCI) has focused on cervical SCI. Reproducible systems have been developed for MRI-based grading; however, it is unclear how they apply to thoracic SCI. Our hypothesis is that MRI measures will group as coherent multivariate principal component (PC) ensembles, and that distinct PCs and individual variables will show discriminant validity for predicting early impairment in thoracic SCI. We undertook a retrospective cohort study of 25 patients with acute thoracic SCI who underwent MRI on admission and had American Spinal Injury Association Impairment Scale (AIS) assessment at hospital discharge. Imaging variables of axial grade, sagittal grade, length of injury, thoracolumbar injury classification system (TLICS), maximum canal compromise (MCC), and maximum spinal cord compression (MSCC) were collected. We performed an analytical workflow to detect multivariate PC patterns followed by explicit hypothesis testing to predict AIS at discharge. All imaging variables loaded positively on PC1 (64.3% of variance), which was highly related to AIS at discharge. MCC, MSCC, and TLICS also loaded positively on PC2 (22.7% of variance), while variables concerning cord signal abnormality loaded negatively on PC2. PC2 was highly related to the patient undergoing surgical decompression. Variables of signal abnormality were all negatively correlated with AIS at discharge with the highest level of correlation for axial grade as assessed with the Brain and Spinal Injury Center (BASIC) score. A multiple variable model identified BASIC as the only statistically significant predictor of AIS at discharge, signifying that BASIC best captured the variance in AIS within our study population. Our study provides evidence of convergent validity, construct validity, and clinical predictive validity for the sampled MRI measures of SCI when applied in acute thoracic and thoracolumbar SCI.

Key words: BASIC; MRI; spinal cord injury; thoracic; T2 hyperintensity; TLICS

Introduction

Acute traumatic spinal cord injury (SCI) involving the thoracic and thoracolumbar spinal cord is considerably less common than cervical SCI with approximately 10% of SCI involving the thoracic spine and another 6% involving the cervicothoracic or thoracolumbar junctions.[1] Most of the literature examining MRI findings in acute traumatic SCI have focused on the more common injury to the cervical spinal cord with relatively little attention given to acute SCI caudal to the cervical level.[2–23] Anatomic and functional distinctions are significant between the cervical and more caudal spinal cord segments, suggesting imaging evaluation may, in fact, be level specific.[24,25]

Since the widespread adoption of magnetic resonance imaging (MRI) in evaluating the spinal cord in the acute setting, there have been numerous studies examining the prognostic value of MRI in acute cervical spinal cord trauma.[2–5,7,9,11–23,26,27] The majority of these studies have focused on the longitudinal extent of T2 signal abnormality in the sagittal plane or secondary markers of SCI, such as canal and spinal cord compression in the cervical spine.[2,3,5,7,9,11–23,26–29] The internal architecture of the spinal cord, however, including the predominant longitudinal orientation of functionally important ascending and descending white matter tracts, would suggest that the transverse extent of injury should be a strong predictor of clinical outcome; this hypothesis has been corroborated by pre-clinical and, more recently, human studies.[4,8,30–35]

Departments of [1]Radiology and Biomedical Imaging, [2]Emergency Medicine, [3]Neurological Surgery, and [4]Anesthesia and Perioperative Care, University of California San Francisco and San Francisco General Hospital, San Francisco, California.
[5]Brain and Spinal Injury Center, San Francisco General Hospital, San Francisco, California.
[6]San Francisco Veteran's Affairs Medical Center, San Francisco, California.

A number of reproducible systems have been developed for MRI-based grading in acute SCI. The most recent addition is a grading system for the axial plane, termed the Brain and Spinal Injury Center (BASIC) score.[4] The BASIC score can be used in combination with other measures, including a commonly used sagittal grading system, the longitudinal extent of T2 signal abnormality, maximum canal compromise (MCC), maximum spinal cord compression (MSCC), and the thoracolumbar injury classification system (TLICS). With the exception of TLICS, these injury classification systems were initially developed for the more common cervical SCI but could have prognostic value throughout the spinal axis. In this study, we aim to evaluate the application of the various MRI grading systems in the setting of acute thoracic SCI.

We applied multidimensional data-driven analytics to the full set of imaging classifications to assess validity of these MRI metrics for thoracic SCI. Our hypothesis is that the BASIC score and the other MRI measures of SCI will group together as coherent multivariate principal component (PC) ensembles, and that distinct PCs (PC1, PC2, etc.) will show discriminant validity for predicting distinct impairment patterns in thoracic and thoracolumbar SCI at the time of patient discharge.

To test this hypothesis, we performed an analytical workflow of data-driven discovery to detect multivariate PC patterns followed by explicit hypothesis testing of whether the PCs and the individual MRI measures predict neurologic impairment at discharge. Multidimensional data-driven analytics (i.e., nonlinear PC analysis [NLPCA]) were applied to explore the multivariate clustering among various MRI measures to determine their convergent validity and discriminant validity.

Linear mixed modeling (LMM) was then applied to assess the relationship of these ensemble MRI measures with the degree of neurologic impairment measured by the American Spinal Injury Association (ASIA) Impairment Scale (AIS) at hospital discharge.[36,37] The results provide evidence of face validity, convergent validity, discriminant validity, construct validity, and clinical predictive validity for multiple MRI measures when applied in acute thoracic SCI.

Methods

Study cohort

We performed an Institutional Review Board and Health Insurance Portability and Accountability Act compliant retrospective cohort study evaluating patients who presented to a Level I trauma center between 2005 and 2012 with acute thoracic or thoracolumbar SCI. Patients were identified using a Department of Neurological Surgery database compiled of patients with a principal diagnosis of SCI (International Classification of Diseases codes 952–957).

Inclusion criteria were: (1) age ≥18 years, (2) thoracic and/or lumbar spine MRI including at minimum sagittal and axial T2 imaging, and (3) documented clinical assessments including AIS at admission and discharge. Exclusion criteria were (1) surgical decompression and/or fusion before MRI, (2) MRI that was too degraded by motion or other artifact such that images were nondiagnostic as assessed by an attending neuroradiologist, (3) cervical spinal cord injury, and (4) injuries primarily involving the conus medullaris or cauda equina nerve roots, (5) pre-existing hardware.

Twenty-five patients met inclusion and exclusion criteria. Clinical data collected included patient age, sex, AIS grade at discharge, time to MRI, time to discharge, mechanism, and whether surgical decompression was performed before hospital discharge (Table 1). All patients in the study cohort had a principal diagnosis of SCI and underwent our institutional SCI treatment protocol. The five patients classified as AIS grade E on formal admission examination had documented symptoms of truncal/lower extremity sensory deficits and/or had documentation of motor weakness in the field. These deficits had resolved AT neurological examination on admission and therefore qualify as AIS grade E.

MRI

All MRI were acquired on a 1.5 Tesla GE Genesis Signa HDxt scanner, software version 15 (GE Healthcare, Milwaukee, WI). Routine trauma protocol thoracic spine MRIs were performed including at minimum sagittal T1 and T2 fast spin echo (FSE) sequences and axial T2 FSE sequences. For sagittal T1 imaging, the following parameters were used: slice thickness = 3 mm; time to repetition (TR) = between 520 msec and 630 msec; time to echo (TE) = between 9 msec and 15 msec; echo train length (ETL) = 3; field-of-view (FOV) = 30 cm^2; acquisition matrix = 512 × 512. For sagittal T2: slice thickness, FOV, and matrix size were as above with TR between 3100 msec and 4000 msec and TE between 105 msec and 120 msec; ETL was between 19 and 21. For axial T2 imaging, slice thickness was 4 mm, TR between 4000 and 4800 msec, TE between 102 and 120 msec, ETL = 25, FOV = 18 cm, and acquisition matrix size = 512 × 512. Additional sequences were performed but not evaluated for the purposes of this study.

Image analysis

A board certified neuroradiologist and a neuroradiology trainee performed independent imaging ratings (Table 2), blinded to clinical outcomes, on retrospectively evaluated imaging sequences (Fig. 1). Any disagreements in categorization were discussed with ultimate deferral to the more experienced reader. The level of injury was defined as the epicenter of largest anterior to posterior extent of

Table 1. Patient Characteristics*

Characteristics	
Age (years)	38.32 ± 15.74
Sex	17 male: 8 female
Injury type	Blunt = 21, penetrating = 4
AIS at admission	A = 11, B = 2, C = 1, D = 6, E = 5
AIS at discharge	A = 9, B = 0, C = 2, D = 5, E = 9
Time to MRI (hours)	14.68 ± 18.56
Time to discharge (days)	20.96 ± 21.48
Surgical decompression before discharge	Yes = 16, No = 9
Mechanism of injury	10 fall from height, 5 motor vehicle collision, 3 crush injuries by large falling objects, 2 gunshot wounds, 2 stab wounds, 1 motorcycle collision
Vertebral body level of epicenter of injury by imaging	1 T2, 1 T3, 1 T4, 3 T6, 2 T7, 3 T8, 2 T9, 1 T11, 7 T12, 3 T1, 1 without detectable injury
BASIC score	1.88 ± 1.67
Sagittal grade	2.32 ± 1.22
Longitudinal extent of injury (mm)	23.52 ± 26.56
TLICS Score	5.16 ± 2.78
MCC (%)	23.38 ± 27.36
MSCC (%)	18.67 ± 24.02

*Results are expressed as N or mean ± standard deviation.

AIS, American Spinal Injury Association (ASIA) Impairment Scale; MRI, magnetic resonance imaging; BASIC, Brain and Spinal Injury Center; TLICS, thoracolumbar injury classification system; MCC, maximum canal compromise; MSCC, maximum spinal cord compression.

Table 2. Magnetic Resonance Imaging Scoring Schemes

Brain and Spinal Injury Center grading system	Ordinal	0–4; 0 = normal, 1 = gray matter only, 2 = some WM, 3 = all WM in plane, 4 = with hemorrhage.
Sagittal grade	Ordinal	1–4; 1 = normal, 2 = less than a vertebral body (VB), 3 = longer than one VB, 4 = with hemorrhage
Longitudinal extent of T2 signal abnormality	Numerical	(mm)
Thoracolumbar injury classification system	Ordinal	Rates: morphology (1–4), neurologic status (0–3), and integrity of the posterior ligamentous complex (0–3)
Maximum canal compromise (MCC)	Numerical	MCC (%) = 1−[Dx/(Da+Db)/2] × 100%; D: canal width
Maximum spinal cord compression (MSCC)	Numerical	MSCC (%) = 1−[dx/(da+db)/2] × 100%; d: spinal cord width

cord signal abnormality on sagittal imaging or as the level of bony injury/canal compromise if there was no cord signal abnormality.

BASIC grading was performed as has been described previously (Fig. 1D) by reviewing the axial images at the epicenter of the injury: briefly, grade 0 injury represented normal spinal cord T2 signal, grade 1 injury represented T2 hyperintensity approximately confined to expected location of spinal gray matter, grade 2 injury represented T2 hyperintensity extending beyond the expected margins of central gray matter and obscuring gray-white margins but not involving the entire transverse extent of the spinal cord (a peripheral rim of normal appearing white matter was identified), grade 3 injury represented T2 hyperintensity involving the entire transverse extent of the spinal cord without any residual normal appearing white matter, and grade 4 injury represented grade 3 injury with superimposed discrete foci of intramedullary T2 hypointensity attributed to the presence of macroscopic intramedullary hemorrhage.[4]

All BASIC scoring was based on a single axial image from the injury epicenter that was determined to have the most severe grade among all axial slices. Sagittal grade was assigned as follows (Fig. 1E): grade 1 represented normal spinal cord signal; grade 2 represented T2 hyperintense intramedullary signal with longitudinal extent confined to a single vertebral level; grade 3 represented >1 vertebral level edema; and grade 4 represented mixed hemorrhage and edema.[2,3]

We also measured the greatest longitudinal extent of injury on sagittal T2 images in mm as described in the SCI common data elements (CDE) version 1.0 (Fig. 1A). MCC and MSCC were also both measured on midsagittal images as described previously, by dividing the anterior-posterior (AP) diameter of the canal (for MCC) and the AP diameter of spinal cord (for MSCC) by the average of the canal or spinal cord above and below as described in the literature with MCC measured on T1 and MSCC measured on T2 (Fig. 1B,C).[11,19,27,29,38] TLICS was assigned as described in the literature after reviewing any necessary computed tomography (CT) imaging and the clinical chart.[39–41]

Multidimensional analytical workflow and statistical analysis

All statistical analyses were performed in SPSS v. 22 (SPSS Inc.; Chicago, IL). To assess the relationship between the different MRI measures, we used a NL-PCA in the general workflow depicted in

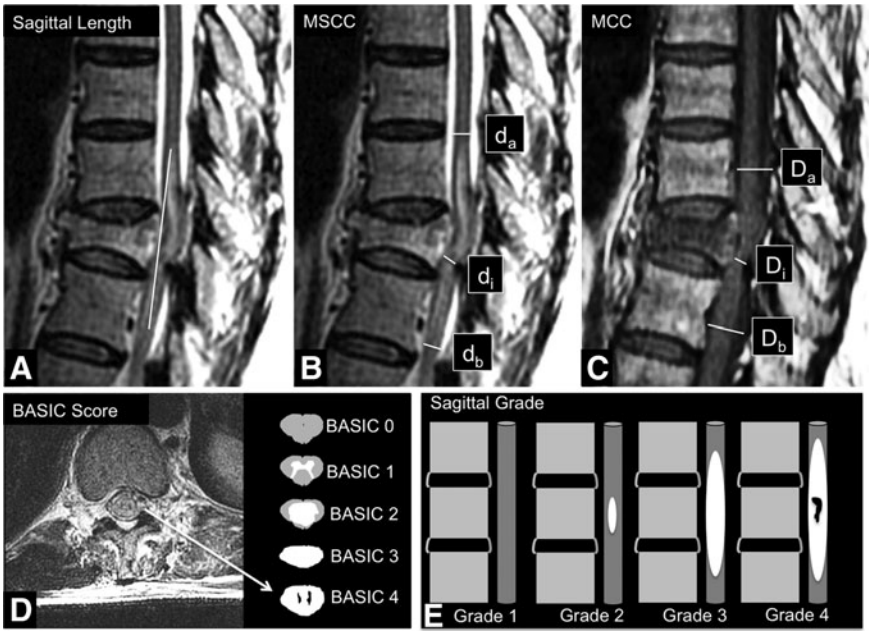

FIG. 1. Image analysis. (**A, B**) Sagittal T2-weighted magnetic resonance imaging (MRI) of the thoracic spine in a patient with acute SCI demonstrating how this sequence was used to measure the length of T2 signal hyperintensity in mm (white line in A) and tocalculate maximum spinal cord compression (MSCC) (B, (1-(d/((da+db)/2)) ×100%). (**C**) Sagittal T1-weighted image of the thoracic spine demonstrating how this sequence was used to measure MCC ((1-(D/((Da+Db)/2)) ×100%). (**D**) Axial T2-weighted MRI of the thoracic spine at the level of the epicenter of injury in a different patient. Foci of T2 hypointense hemorrhage are surrounded by hyperintense edema with no normal cord signal, consistent with BASIC grade 4; white arrow denotes associated cartoon depiction of Brain and Spinal Injury Center (BASIC) axial grade. (**E**) Cartoon of the sagittal grading system.

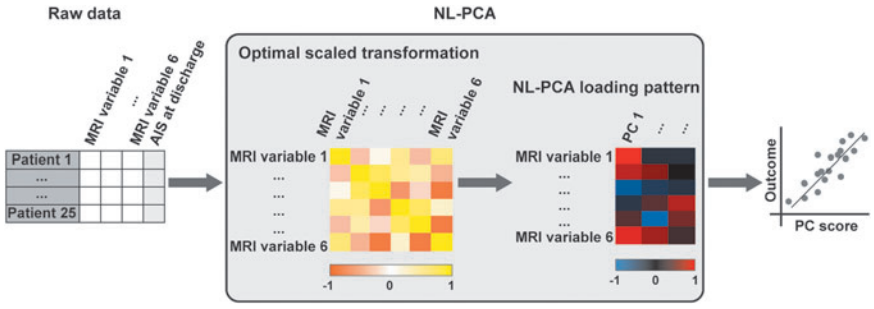

FIG. 2. Multidimensional analytical workflow. Raw magnetic resonance imaging (MRI) variables are fed into a nonlinear principal component analysis (NL-PCA). NL-PCA uses a process called optimal scaling transformation to handle different analysis levels (e.g., ordinal and numeric) in the dataset. Optimal scaling assigns quantitative values to categorical variables optimally, meaning maximizing the variance of the predefined number of principal components (PCs) (i.e., dimensions). The NL-PCA loading pattern shows the weight (i.e., loading) of every single MRI variable on the extracted PCs. In a next step, individual PC scores are used to define the predictive nature of PCs on outcome. An individual PC score is the sum of the multiplied loadings by the individual raw value of every single variable. AIS, American Spinal Injury Association (ASIA) Impairment Scale. Color image is available online at www.liebertpub.com/neu

Figure 2. NL-PCA is suitable for a set of variables including mixed measurement levels (nominal, ordinal, and numeric).[42,43] In NL-PCA, variables are assigned numerical values through an automated process called optimal scaling transformation. First, NL-PCA was applied using a six-dimensional solution. The final dimensionality (i.e., number of PCs) of the PCA was defined based on (1) Kaiser rule: eigenvalue >1 and (2), Cattell rule: scree plot.[44,45] The NL-PCA was then pruned with reduced PC dimensions.

To determine the stability of the NL-PCA solution, we performed a nonparametric balanced bootstrapping procedure using 2000 iterations and Procrustes rotation.[46] The two-dimensional NL-PCA solution was further cross-validated with the bootstrapped solution by using root mean square difference in PC loading patterns, the coefficient of congruence, the Pearson product moment correlation coefficient, and the Cattell salient variable similarity index. Convergence of these mathematically distinct metrics indicates consensus for replication of PC patterns.

The sensitivity of the extracted two-dimensional PC scores for predicting AIS at discharge was tested with a linear mixed model. To assess the bivariate relationship between AIS at discharge and MRI measures, separate Spearman rank correlations and an optimal scaled regression were applied. These procedures allow a direct comparison between the univariate correlations from individual variables and multivariable sets with different metric features (i.e., ordinal and numeric).

All predictive validity testing was based on individual MRI measures from MRI obtained near time of admission and AIS at time of patient discharge from the hospital. Statistical significance for all analysis was set at $\alpha = 0.05$. Bootstrapping and power calculations indicated that the $N = 25$ was sufficient for assessing the predictive validity of MRI with respect to AIS at discharge.

Levels of validity

Validation of MRI measures involves different levels of validity assessment as described by classical measurement theory. ''Face validity'' is defined as the concept that the MRI measures accurately reflect what they purport to measure on face value (i.e., an MRI-measured lesion looks like a lesion). ''Convergent validity'' is the concept that measures that should correlate, do indeed correlate (i.e., lesion length and lesion area do correlate). ''Discriminant validity'' refers to the concept that measures that should diverge, do indeed diverge (i.e., measures of ligamentous change diverge from neuroanatomical measures). ''Construct validity'' refers to the concept that multidimensional patterns are coherent from a theoretical perspective (i.e., neuroscores coalesce as coherent unit). Construct validity can be considered to involve both discriminant and convergent validity. ''Predictive validity'' refers to the concept that multidimensional MRI patterns can predict outcome. In the Results section, we address which level of validity is addressed by each statistical finding.

Results

Patient characteristics, MRI metrics, and TLICS scores for our cohort are presented in Table 1. Optimally scaled correlation revealed strong bivariate associations among MRI measures (Fig. 3A). NL-PCA analysis revealed that PC1–3 had high loadings by MRI scores (Fig. 3B). The Cattell and Kaiser criteria for PC retention converged on retention of a pruned two-dimensional PC solution (Fig. 3C). Re-extraction of NL-PCA restricted to two dimensions confirmed that PC1–2 accounted for 87.0% of the variance (64.3% and 22.7%, respectively) in imaging findings (Fig. 3D).

The bootstrapping results support the stability of the two-dimensional PCA solutions with only marginal changes in the total variance accounted for (total: 89.4%; PC1: 64.3%; PC2: 25.1%). Further, the loading pattern of the two-dimensional NL-PCA strongly agrees with the loading pattern of the bootstrapped PCA solution for both PC1 (root mean square difference = 0, coefficient of congruence = 1, Pearson product moment correlation coefficient = 1, and Cattell salient variable similarity index = 1, $p < 0.05$) and PC2 (root mean square difference = 0, coefficient of congruence = 1, Pearson product moment correlation coefficient = 1, and Cattell salient variable similarity index = 0.86, $p < 0.05$).

In the two-dimensional NL-PCA solution, all imaging variables loaded positively on PC1. MCC, MSCC, and TLICS also loaded positively on PC2 (variance orthogonal to PC1) while BASIC, sagittal grade, and longitudinal extent of injury loaded negatively on PC2. Together these results suggest that the PC1–2 reflect radiological tissue changes (face validity); that PC1 reflects agreement among MRI scoring schemes (convergent validity); and that PC1 and PC2 reflect distinct patterns, with PC2 reflecting divergence among two distinct blocks of scoring schemes (discriminant validity).

To better understand the discriminant nature of PC2, we projected individual patients into the PC1–PC2 biplot space (Fig. 4) and discovered that there appeared to be a broad dispersion of subjects within the PC space, suggesting the potential for distinct subpopulations. We hypothesized that spinal decompression surgery may account for the dissociations among patient distributions. Linear mixed model regression confirmed that spinal decompression

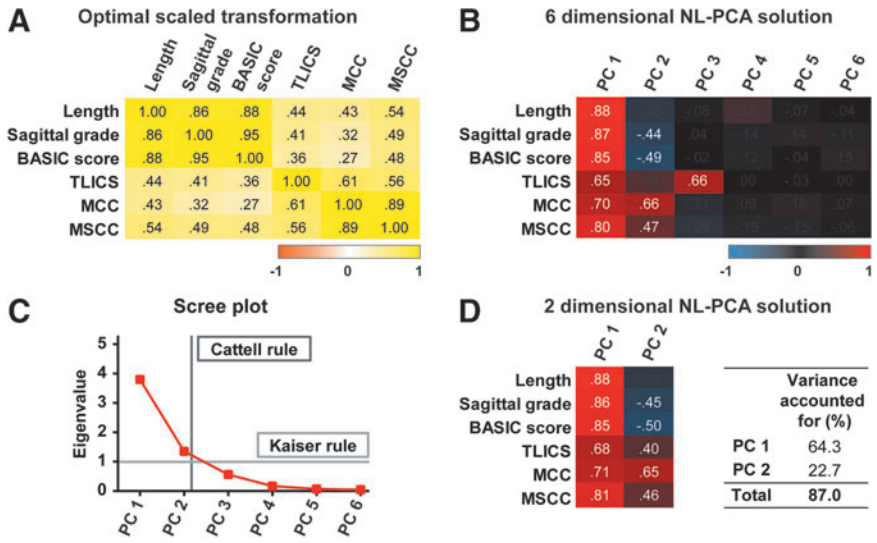

FIG. 3. Non-linear principal component analysis (NL-PCA) results demonstrate face validity, convergent validity, and construct validity. (**A**) Optimal scaled transformation matrix of all magnetic resonance imaging measures. (**B**) Six-dimensional NL-PCA solution loading patterns. Loadings $\geq|0.4|$ are emphasized in white. (**C**) Shows the scree plot for the six-dimensional NL-PCA. The Cattell and the Kaiser rules were applied to define the amount of components to retain for the final NL-PCA. The criteria converged on a two-dimensional solution, (**D**) Shows the re-extracted two-dimensional NL-PCA solution and the amount of variance accounted for by the two principal components (PCs). Loading values $\geq|0.4|$ are in white text. BASIC score, Brain and Spinal Injury Center score; TLICS, thoracolumbar injury classification system; MCC, maximum canal compromise; MSCC, maximum spinal cord compression. Color image is available online at www.liebertpub.com/neu

impacted PC2 scores ($F=25.4$, $p<0.0001$) but not PC1 ($p>0.05$). This suggests that PC2 may reflect MRI features associated with the clinical decision making process to perform spinal cord decompression. Careful re-examination of the loadings further supports this idea (Fig. 3D).

To test the predictive validity of PC1 and PC2 MRI ensembles, we used mixed model regression to test their association with AIS at discharge. Both PC1 and PC2 were statistically significantly related to AIS at discharge (PC1: $F=8.63$, $p=0.001$, eta squared $=0.55$, power $=0.98$; PC2: $F=3.28$, $p=0.041$, eta squared $=0.32$, power $=0.66$). PC1 specifically predicted AIS neurological impairment at time of patient discharge across the range of injuries in a monotonic fashion, with higher PC1 scores reflecting worse function (AIS A) and lower PC1 scores reflecting better function (AIS E) ($p<0.05$ by linear contrast; $p>0.05$ for quadratic).

PC2, on the other hand, had a narrower range of association with neurologic impairment, differentiating AIS A from other AIS grades ($p<0.05$) with no other statistical significance. Because of the retrospective nature of the study, AIS at discharge was chosen as the short-term outcome. To assess the relationship between PC1/PC2 and length of stay, a Pearson correlation was performed (PC1: Pearson $r=0.45$, $p=0.023$, and PC2 $r=-0.39$, $p=0.057$); this indicates that multidimensional MRI predicts length of stay, as a secondary validation end point.

To better understand the predictive validity of the individual MRI scores versus the PC1 and PC2 ensembles, we performed a nonparametric Spearman rank correlations of imaging variables with AIS at discharge (Table 3 and Fig. 5). BASIC score (rho $=-0.93$), sagittal grade (rho $=-0.85$), longitudinal extent of injury (rho $=-0.83$), and PC1 (rho $=-0.75$) were all negatively correlated with AIS at discharge. PC2 (rho $=0.49$) was mildly positively correlated with AIS at discharge, while TLICS, MCC, and MSCC were not statistically significantly correlated with AIS at discharge.

To confirm the comparative predictive validity results, we used an optimal scaled regression. This method provides a way to compare correlations between variables with different properties and distributions. BASIC was the only statistically significant ($p=0.001$) predictor of AIS at discharge in this multiple variable model. Because of multicolinearity, PC1 and PC2 were not included in the optimal scaling regression.

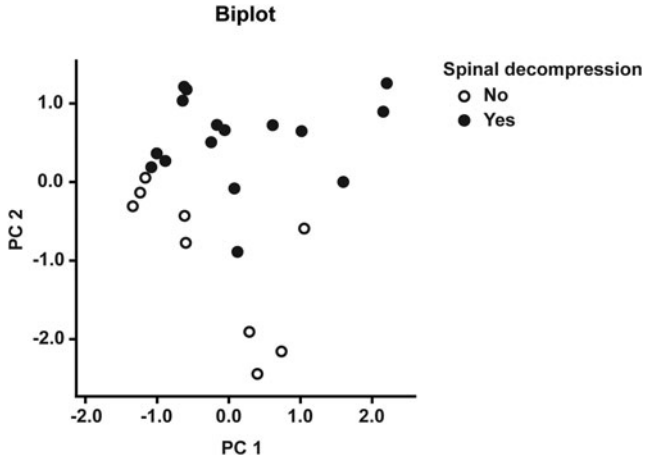

FIG. 4. Discriminant validity of principal component 2 (PC2). Individual subject's PC scores are plotted into the two-dimensional biplot space described by PC1 and PC2. Subjects who underwent surgical decompression (closed circles) after magnetic resonance imaging acquisition have higher PC2 scores than those who did not (open circles). The biplot highlights the discriminative validity of PC2.

Discussion

In this study, we assessed multiple MRI metrics of SCI, which were all predominately developed for use in the more common cervical SCI, here applied in thoracic SCI. TLICS, which is an

Table 3. Spearman Rank Correlation and Optimal Scaling Regression to Predict American Spinal Injury Association (ASIA) Impairment Scale at Discharge*

	Spearman correlation			*Optimal scaling regression*			
	Rho	*Rho squared*	*Sig*	*Zero-order*	*Partial*	*Part*	*Sig*
Length	–0.83	0.68	<0.001	–0.81	–0.09	–0.02	0.859
Sagittal grade	–0.85	0.73	<0.001	–0.67	0.65	0.16	0.514
BASIC score	–0.93	0.86	<0.001	–0.96	–0.92	–0.44	0.001
TLICS	–0.21	0.04	0.323	–0.11	–0.64	–0.15	0.203
MCC	–0.04	0.00	0.850	–0.17	0.30	0.06	0.405
MSCC	–0.20	0.04	0.351	–0.40	0.06	0.01	0.862
PC1	–0.75	0.57	<0.001				
PC2	0.49	0.24	0.014				

*Length of signal abnormality, sagittal grade, Brain and Spinal Injury Center (BASIC) score, and principal component (PC)1 are all negatively correlated with AIS at discharge while PC2 is positively correlated with American Spinal Injury Association (ASIA) Impairment Scale (AIS) at discharge. Optimal scaling regression identified BASIC score as the only statistically significant variable in this multiple variable model to predict AIS at discharge.

TLICS, thoracolumbar injury classification system; MCC, maximum canal compromise; MSCC, maximum spinal cord compression.

injury classification system for surgical decision making in thoracic spinal column injury and not a prognostic system, was also included to evaluate its relationship with the other imaging variables. TLICS does incorporate clinical data related to patient neurologic status in addition to imaging findings.

We used nonlinear principal components analysis to characterize the relationships of these variables and found two PCs accounting for 87.0% of the variance. All imaging variables loaded positively on PC1 (64.3% of the variance), which was highly related to AIS at discharge. MCC, MSCC, and TLICS also loaded positively on PC2 (22.7% of the variance), while variables concerning spinal cord signal abnormality loaded negatively on PC2. We found that PC2 was highly related to the patient undergoing surgical decompression.

BASIC, sagittal grade, and longitudinal extent of signal abnormality were all negatively correlated with AIS at discharge with the highest individual level of correlation for BASIC. In a multiple variable model, BASIC was the only statistically significant predictor of AIS at discharge, demonstrating that it most accurately predicted the variance of AIS at discharge in our study population. Our study provides evidence of convergent validity, construct validity, and clinical predictive validity for these imaging predominant measures of SCI when applied in acute thoracic SCI.

Variables involving spinal cord signal abnormality are highly related to each other and to AIS at discharge. By definition, these three variables are similar because they primarily consider the presence or absence of T2 signal hyperintensity in the spinal cord. The axial grading system (BASIC) and the sagittal grading system differ in their mild to moderate grades and direction of significance; however, both consider hemorrhage superimposed on edema as the highest grade. Otherwise, in the mild to moderate grades, BASIC is primarily concerned with the degree of spared white matter and the sagittal grading system is primarily concerned with single vertebral level versus multiple vertebral level edema. The sagittal grading

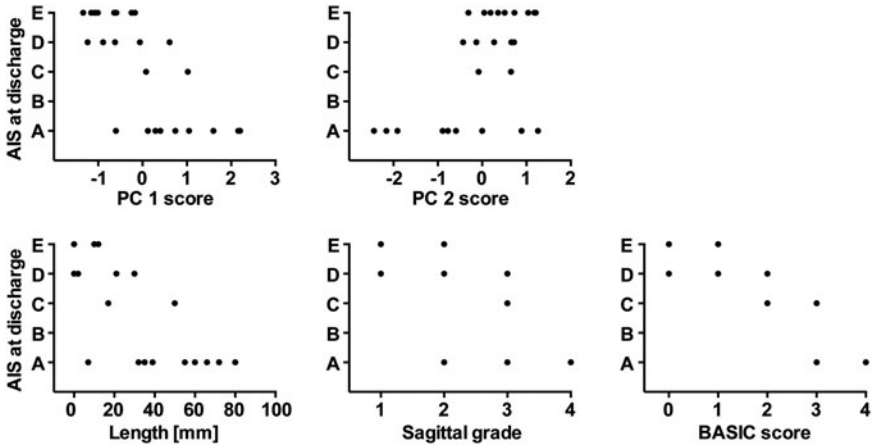

FIG. 5. Predictive validity. Scatterplots of American Spinal Injury Association (ASIA) Impairment Scale (AIS) at discharge with each statistically significant variable. Brain and Spinal Injury Center (BASIC) score had the highest individual level of individual correlation with AIS at discharge. BASIC score (rho = –0.927), sagittal grade (rho = –0.852), longitudinal extent of injury (rho = –0.825), and principal component (PC)1 (rho = –0.753) were all negatively correlated with AIS at discharge. PC2 (rho = 0.486) was mildly positively correlated with AIS at discharge, while thoracolumbar injury classification system, maximum canal compromise, and maximum spinal cord compression were not statistically significantly correlated with AIS at discharge. Note that because of the ordinal scale of the sagittal grade and the BASIC score, a number of subjects coincide on both x and y axes.

system (ordinal) and the longitudinal extent of T2 signal abnormality (numerical) are by definition similar concepts except that the sagittal grade also accounts for the presence of hemorrhage.

As expected, these variables grouped together on PC analysis and were positively correlated together providing evidence of convergent and construct validity and were negatively correlated with AIS at discharge providing evidence of clinical predictive validity. BASIC demonstrated the highest individual degree of negative correlation with AIS at discharge; however, all three metrics can be considered individually valid for predicting early neurological impairment in thoracic SCI.

The multiple variable model identified BASIC as the dominant imaging variable in predicting AIS at discharge, because it was the only statistically significant variable in the multiple regression model. This suggests that BASIC (a brief ordinal scale) most tightly captures AIS (also a brief ordinal scale) at discharge compared with the other measures.

MCC, MSCC, and TLICS grouped together with the other imaging variables on PC1 but diverged from the other imaging variables (of spinal cord signal abnormality) on PC2. Because PC2 was highly related to the patient undergoing spinal decompression and positively correlated with AIS at discharge, the relationship of these variables that loaded positively on PC2 (MCC, MSCC, TLICS) with AIS at discharge is thus quite complex. These three variables have variance with PC1 correlating negatively with AIS at discharge, and variance with PC2 correlating positively with AIS at discharge and being highly related to the likelihood of undergoing surgical decompression.

PC2 thus may capture some of the nuances of surgical decision-making reflected in TLICS whereby an incomplete SCI at admission receives a higher individual scoring than a complete SCI. The particular phenotype captured by a high PC2 score would be a patient with a high MCC, MSCC, and TLICS but lower scores on measures of cord signal abnormality; a patient with an unstable spine and compression but a relatively preserved spinal cord.

The fact that MCC and MSCC did not individually have a significant correlation with AIS at discharge is consistent with previous literature examining measures of spinal canal stenosis with thoracolumbar SCI outcomes and may reflect the complexity of their relationship with both surgical decision making and subsequent early neurological impairment.[47] The strong negative correlations between direct MRI measures of SCI (BASIC score, sagittal grade, and longitudinal length of T2 signal hyperintensity) and clinical outcomes suggests incorporation of these measures into surgical decision-making tools may be helpful. Defining valid imaging biomarkers for thoracic and thoracolumbar SCI is critically important because the thoracic spinal cord has been proposed as the most suitable region for initial invasive clinical trials targeting SCI.[48,49]

Our study has several limitations mostly related to the retrospective technique and relatively small sample size. Our retrospective technique allowed us to effectively study the relatively rare thoracic SCI in an efficient manner but did limit the clinical variables to those already collected in routine clinical care. The retrospective nature of this study also limits our control over timing of MRI after injury.

Leypold and colleagues[50] have shown that the longitudinal extent of T2 hyperintensity can increase by up to one vertebral body height per day in the acute stage of injury. Our institution routinely obtains MRI early after injury, and 88% (22/25) were performed within 24 h of injury, thus limiting the effect of delayed timing on extent of T2 hyperintensity. Future prospective controlled experiments would ideally control for variables such as hemodynamic support, timing of surgical decompression, steroid therapy, and timing of MRI after injury with longer-term clinical follow-up and a larger number of patients. Importantly, our study does suggest that any prospective collection of data in thoracic SCI should include metrics of spinal cord signal abnormality on MRI as measured in this study.

Another limiting factor is the use of AIS grade as a fairly coarse primary outcome measure for thoracic SCI in our cohort. Because of the retrospective nature of this study, more granular outcome measures, such as functional independence measure (FIM), were not available for analysis. Although the significance of AIS grade has been questioned in thoracic SCI, Lee and colleagues[51] recently showed that AIS grade changes are associated with significant functional benefit relative to FIM scores and ambulation in a retrospective analysis of a large longitudinal database of patients with thoracic SCI.[52]

Structural MRI findings correlated with early impairment with varying resolution, depending on the scoring scheme (e.g., BASIC vs. sagittal grade). Multiple regression analysis confirmed that most of the univariate MRI assessments were noisy correlates of functional impairment, with the sole exception of the BASIC score. In testing theory, this class of evidence is referred to as predictive validity, and it directly addresses whether a set of measurements (MRI features) have value for predicting a separate outcome domain (AIS grade) at a later time.

Our application of NL-PCA directly assessed whether the multidimensional ensemble of spinal cord MRI features performs better than each individual outcome. NL-PCA is a rigorous and appropriate approach for performing multivariate pattern-detection to compare the relative merits of multiple scales that purport to measure the same underlying features (in this case, structural MRI features). This approach has a long history in physics, human performance testing, and other disciplines dating back more than a century.[53,54]

Although it is currently unusual to have such advanced analytics applied in the clinic, applications like the one here promise to be a central feature of the emerging field of ''precision medicine,'' where analytics will be integrated in clinical decision making.[55,56] Accordingly, several very recent articles incorporate NL-PCA as a precision medicine tool in both pre-clinical and clinical SCI.[57–59] The present findings suggest that multidimensional MRI features of the thoracic spinal cord may have relevance for clinical issues such as patient stratification for diagnosis, intervention planning, and clinical trial criteria. Further work is needed, however, to test the capacity of structural MRI to predict long-term outcome.

Conclusion

This study validates the use of BASIC and other MRI measures of acute SCI specifically in the setting of thoracic SCI. PC analysis identified two distinct patterns of variance: PC1, which was highly related to AIS at discharge, and PC2, which was highly related to surgical decompression. The highest individual correlation with AIS at discharge was seen with the BASIC system, although all metrics of spinal cord signal abnormality had a high degree of individual negative correlation with AIS at discharge. The relationship of MCC and MSCC with AIS at discharge was found to be more complex, likely reflecting the use of these metrics along with TLICS in surgical decision making. A multiple variable regression model identified BASIC as the only statistically significant predictor of AIS at discharge, signifying that BASIC best captured the variance in AIS within our study population.

Acknowledgment

This work was supported by R01NS067092 (ARF), the Craig H. Neilsen Foundation (ARF; JCB), Wings for Life Foundation (ARF), DOD grant CDMRP SCIRP 120559 (W81XWH-13-1-0297) (MSB and JCB). MCM was supported by an NIH T32 Fellowship, 5T32EB001631-10. JH was supported by a Craig H. Neilsen Foundation fellowship (313739).

Author Disclosure Statement

Dr. Talbott is a member of the data monitoring committee for StemCells, Inc.; Dr. Ferguson is an *ad hoc* consultant for Acorda Therapeutics. For the remaining authors, no competing financial interests exist.

References

1. Pickett, G.E., Campos-Benitez, M., Keller, J.L., and Duggal, N. (2006). Epidemiology of traumatic spinal cord injury in Canada. Spine (Phila Pa 1976) 31, 799–805.
2. Bozzo, A., Marcoux, J., Radhakrishna, M., Pelletier, J., and Goulet, B. (2011). The role of magnetic resonance imaging in the management of acute spinal cord injury. J. Neurotrauma 28, 1401–1411.
3. Bondurant, F.J., Cotler, H.B., Kulkarni, M.V., McArdle, C.B., and Harris, J.H., Jr. (1990). Acute spinal cord injury. A study using physical examination and magnetic resonance imaging. Spine (Phila Pa 1976) 15, 161–168.
4. Talbott, J.F., Whetstone, W.D., Readdy, W.J., Ferguson, A.R., Bresnahan, J.C., Saigal, R., Hawryluk, G.W., Beattie, M.S., Mabray, M.C., Pan, J.Z., Manley, G.T., and Dhall, S.S. (2015). The Brain and Spinal Injury Center score: a novel, simple, and reproducible method for assessing the severity of acute cervical spinal cord injury with axial T2-weighted MRI findings. J. Neurosurg. Spine 23, 495–504.
5. Shimada, K., and Tokioka, T. (1999). Sequential MR studies of cervical cord injury: correlation with neurological damage and clinical outcome. Spinal Cord 37, 410–415.
6. Shen, H., Tang, Y., Huang, L., Yang, R., Wu, Y., Wang, P., Shi, Y., He, X., Liu, H., and Ye, J. (2007). Applications of diffusion-weighted MRI in thoracic spinal cord injury without radiographic abnormality. Int. Orthop. 31, 375–383.
7. Schaefer, D.M., Flanders, A., Northrup, B.E., Doan, H.T., and Osterholm, J.L. (1989). Magnetic resonance imaging of acute cervical spine trauma. Correlation with severity of neurologic injury. Spine (Phila Pa 1976) 14, 1090–1095.
8. Rao, J.S., Zhao, C., Yang, Z.Y., Li, S.Y., Jiang, T., Fan, Y.B., and Li, X.G. (2013). Diffusion tensor tractography of residual fibers in traumatic spinal cord injury: A pilot study. J. Neuroradiol 40, 181–186.
9. Ramon, S., Dominguez, R., Ramirez, L., Paraira, M., Olona, M., Castello, T., and Garcia Fernandez, L. (1997). Clinical and magnetic resonance imaging correlation in acute spinal cord injury. Spinal Cord 35, 664–673.
10. Pouw, M.H., van der Vliet, A.M., van Kampen, A., Thurnher, M.M., van de Meent, H., and Hosman, A.J. (2012). Diffusion-weighted MR imaging within 24 h post-injury after traumatic spinal cord injury: a qualitative meta-analysis between T2-weighted imaging and diffusion-weighted MR imaging in 18 patients. Spinal Cord 50, 426–431.
11. Miyanji, F., Furlan, J.C., Aarabi, B., Arnold, P.M., and Fehlings, M.G. (2007). Acute cervical traumatic spinal cord injury: MR imaging findings correlated with neurologic outcome—prospective study with 100 consecutive patients. Radiology 243, 820–827.
12. Mihai, G., Nout, Y.S., Tovar, C.A., Miller, B.A., Schmalbrock, P., Bresnahan, J.C., and Beattie, M.S. (2008). Longitudinal comparison of two severities of unilateral cervical spinal cord injury using magnetic resonance imaging in rats. J. Neurotrauma 25, 1–18.
13. Marciello, M.A., Flanders, A.E., Herbison, G.J., Schaefer, D.M., Friedman, D.P., and Lane, J.I. (1993). Magnetic resonance imaging related to neurologic outcome in cervical spinal cord injury. Arch. Phys. Med. Rehabil. 74, 940–946.
14. Kulkarni, M.V., McArdle, C.B., Kopanicky, D., Miner, M., Cotler, H.B., Lee, K.F., and Harris, J.H. (1987). Acute spinal cord injury: MR imaging at 1.5 T. Radiology 164, 837–843.
15. Kulkarni, M.V., Bondurant, F.J., Rose, S.L., and Narayana, P.A. (1988). 1.5 tesla magnetic resonance imaging of acute spinal trauma. Radiographics 8, 1059–1082.
16. Kalfas, I., Wilberger, J., Goldberg, A. and Prostko, E.R. (1988). Magnetic resonance imaging in acute spinal cord trauma. Neurosurgery 23, 295–299.
17. Flanders, A.E., Spettell, C.M., Tartaglino, L.M., Friedman, D.P., and Herbison, G.J. (1996). Forecasting motor recovery after cervical spinal cord injury: value of MR imaging. Radiology 201, 649–655.
18. Flanders, A.E., Spettell, C.M., Friedman, D.P., Marino, R.J., and Herbison, G.J. (1999). The relationship between the functional abilities of patients with cervical spinal cord injury and the severity of damage revealed by MR imaging. AJNR Am. J. Neuroradiol. 20, 926–934.
19. Fehlings, M.G., Rao, S.C., Tator, C.H., Skaf, G., Arnold, P., Benzel, E., Dickman, C., Cuddy, B., Green, B., Hitchon, P., Northrup, B., Sonntag, V., Wagner, F., and Wilberger, J. (1999). The optimal radiologic method for assessing spinal canal compromise and cord compression in patients with cervical spinal cord injury. Part II: Results of a multicenter study. Spine (Phila Pa 1976) 24, 605–613.
20. Cotler, H.B., Kulkarni, M.V., and Bondurant, F.J. (1988). Magnetic resonance imaging of acute spinal cord trauma: preliminary report. J. Orthop. Trauma 2, 1–4.
21. Collignon, F., Martin, D., Lenelle, J., and Stevenaert, A. (2002). Acute traumatic central cord syndrome: magnetic resonance imaging and clinical observations. J. Neurosurg. 96, 29–33.
22. Chakeres, D.W., Flickinger, F., Bresnahan, J.C., Beattie, M.S., Weiss, K.L., Miller, C., and Stokes, B.T. (1987). MR imaging of acute spinal cord trauma. AJNR Am. J. Neuroradiol. 8, 5–10.
23. Andreoli, C., Colaiacomo, M.C., Rojas Beccaglia, M., Di Biasi, C., Casciani, E., and Gualdi, G. (2005). MRI in the acute phase of spinal cord traumatic lesions: Relationship between MRI findings and neurological outcome. Radiol. Med. 110, 636–645.
24. Harrop, J.S., Maltenfort, M.G., Geisler, F.H., Coleman, W., Jones, L.A., Wirth, E., and Vaccaro, A. (2009). Traumatic thoracic ASIA A examinations and potential for clinical trials. Spine (Phila Pa 1976) 34, 2525–2529.
25. Kingwell, S.P., Noonan, V.K., Fisher, C.G., Graeb, D.A., Keynan, O., Zhang, H., and Dvorak, M.F. (2010). Relationship of neural axis level of injury to motor recovery and health-related quality of life in patients with a thoracolumbar spinal injury. J. Bone Joint Surg. Am. 92, 1591–1599.
26. Freund, P., Weiskopf, N., Ashburner, J., Wolf, K., Sutter, R., Altmann, D.R., Friston, K., Thompson, A., and Curt, A. (2013). MRI investigation of the sensorimotor cortex and the corticospinal tract after acute spinal cord injury: a prospective longitudinal study. Lancet Neurol. 12, 873–881.
27. Fehlings, M.G., Furlan, J.C., Massicotte, E.M., Arnold, P., Aarabi, B., Harrop, J., Anderson, D.G., Bono, C.M., Dvorak, M., Fisher, C., France, J., Hedlund, R., Madrazo, I., Nockels, R., Rampersaud, R., Rechtine, G., Vaccaro, A.R., and Spine Trauma Study Group. (2006). Interobserver and intraobserver reliability of maximum canal compromise and spinal cord compression for evaluation of acute traumatic cervical spinal cord injury. Spine (Phila Pa 1976) 31, 1719–1725.
28. Rao, S.C., and Fehlings, M.G. (1999). The optimal radiologic method for assessing spinal canal compromise and cord compression in patients with cervical spinal cord injury. Part I: An evidence-based analysis of the published literature. Spine (Phila Pa 1976) 24, 598–604.
29. Furlan, J.C., Fehlings, M.G., Massicotte, E.M., Aarabi, B., Vaccaro, A.R., Bono, C.M., Madrazo, I., Villanueva, C., Grauer, J.N., and Mikulis, D. (2007). A quantitative and reproducible method to assess cord compression and canal stenosis after cervical spine trauma: a study of interrater and intrarater reliability. Spine (Phila Pa 1976) 32, 2083–2091.
30. Budde, M.D., Kim, J.H., Liang, H.F., Russell, J.H., Cross, A.H., and Song, S.K. (2008). Axonal injury detected by in vivo diffusion tensor imaging correlates with neurological disability in a mouse model of multiple sclerosis. NMR Biomed. 21, 589–597.
31. Bresnahan, J.C., Beattie, M.S., Stokes, B.T. and Conway, K.M. (1991). Three-dimensional computer-assisted analysis of graded contusion lesions in the spinal cord of the rat. J. Neurotrauma 8, 91–101.
32. Tator, C.H. and Koyanagi, I. (1997). Vascular mechanisms in the pathophysiology of human spinal cord injury. J. Neurosurg. 86, 483–492.
33. Griffin, J.F., Davis, M.C., Ji, J.X., Cohen, N.D., Young, B.D. and Levine, J.M. (2015). Quantitative magnetic resonance imaging in a

naturally occurring canine model of spinal cord injury. Spinal Cord 53, 278–284.
34. Kelley, B.J., Harel, N.Y., Kim, C.Y., Papademetris, X., Coman, D., Wang, X., Hasan, O., Kaufman, A., Globinsky, R., Staib, L.H., Cafferty, W.B., Hyder, F. and Strittmatter, S.M. (2014). Diffusion tensor imaging as a predictor of locomotor function after experimental spinal cord injury and recovery. J. Neurotrauma 31, 1362–1373.
35. Kim, J.H., Loy, D.N., Wang, Q., Budde, M.D., Schmidt, R.E., Trinkaus, K. and Song, S.K. (2010). Diffusion tensor imaging at 3 hours after traumatic spinal cord injury predicts long-term locomotor recovery. J. Neurotrauma 27, 587–598.
36. American Spinal Injury Association. and International Spinal Cord Society. (2006). International standards for neurological classification of spinal cord injury. 6th ed. American Spinal injury Association; International Spinal Cord Society: Chicago, Ill.
37. Kirshblum, S.C., Burns, S.P., Biering-Sorensen, F., Donovan, W., Graves, D.E., Jha, A., Johansen, M., Jones, L., Krassioukov, A., Mulcahey, M.J., Schmidt-Read, M. and Waring, W. (2011). International standards for neurological classification of spinal cord injury (revised 2011). J. Spinal Cord Med. 34, 535–546.
38. Biering-Sorensen, F., Alai, S., Anderson, K., Charlifue, S., Chen, Y., DeVivo, M., Flanders, A.E., Jones, L., Kleitman, N., Lans, A., Noonan, V.K., Odenkirchen, J., Steeves, J., Tansey, K., Widerstrom-Noga, E., and Jakeman, L.B. (2015). Common data elements for spinal cord injury clinical research: a National Institute for Neurological Disorders and Stroke project. Spinal Cord 53, 265–277.
39. Vaccaro, A.R., Lehman, R.A., Jr., Hurlbert, R.J., Anderson, P.A., Harris, M., Hedlund, R., Harrop, J., Dvorak, M., Wood, K., Fehlings, M.G., Fisher, C., Zeiller, S.C., Anderson, D.G., Bono, C.M., Stock, G.H., Brown, A.K., Kuklo, T., and Oner, F.C. (2005). A new classification of thoracolumbar injuries: the importance of injury morphology, the integrity of the posterior ligamentous complex, and neurologic status. Spine (Phila Pa 1976) 30, 2325–2333.
40. Patel, A.A., and Vaccaro, A.R. (2010). Thoracolumbar spine trauma classification. J. Am. Acad. Orthop. Surg. 18, 63–71.
41. Patel, A.A., Dailey, A., Brodke, D.S., Daubs, M., Harrop, J., Whang, P.G., Vaccaro, A.R., and Spine Trauma Study Group. (2009). Thoracolumbar spine trauma classification: the Thoracolumbar Injury Classification and Severity Score system and case examples. J. Neurosurg. Spine 10, 201–206.
42. Linting, M., Meulman, J.J., Groenen, P.J., and van der Koojj, A.J. (2007). Nonlinear principal components analysis: introduction and application. Psychol. Methods 12, 336–358.
43. Linting, M., and van der Kooij, A. (2012). Nonlinear principal components analysis with CATPCA: a tutorial. J. Pers. Assess. 94, 12–25.
44. Kaiser, H.F. (1960). The Application of Electronic Computers to Factor Analysis. Educ. Psychol. Meas. 20, 141–151.
45. Cattell, R.B. (1966). The Scree Test for the number of factors. Multivariate Behav. Res. 1, 245–276.
46. Linting, M., Meulman, J.J., Groenen, P.J., and van der Kooij, A.J. (2007). Stability of nonlinear principal components analysis: an empirical study using the balanced bootstrap. Psychol. Methods 12, 359–379.
47. Dai, L.Y., Wang, X.Y., and Jiang, L.S. (2007). Neurologic recovery from thoracolumbar burst fractures: is it predicted by the amount of initial canal encroachment and kyphotic deformity? Surg. Neurol. 67, 232–238.
48. Reier, P.J., Lane, M.A., Hall, E.D., Teng, Y.D., and Howland, D.R. (2012). Translational spinal cord injury research: preclinical guidelines and challenges. Handb. Clin. Neurol. 109, 411–433.
49. Fawcett, J. (2002). Repair of spinal cord injuries: where are we, where are we going? Spinal cord 40, 615–623.
50. Leypold, B.G., Flanders, A.E., and Burns, A.S. (2008). The early evolution of spinal cord lesions on MR imaging following traumatic spinal cord injury. AJNR Am. J. Neuroradiol. 29, 1012–1016.
51. Lee, B.A., Leiby, B.E., and Marino, R.J. (2014). Neurological and functional recovery after thoracic spinal cord injury. J. Spinal Cord Med. Epub ahead of print.
52. van Middendorp, J.J., Hosman, A.J., Pouw, M.H., EM-SCI Study Group, and Van de Meent, H. (2009). ASIA impairment scale conversion in traumatic SCI: is it related with the ability to walk? A descriptive comparison with functional ambulation outcome measures in 273 patients. Spinal Cord 47, 555–560.
53. Pearson, K. (1901). On lines and points of closest fit to systems of points in space. Philosophical Magazine 2, 559–572.
54. Spearman, C. (1904). ''General intelligence'' objectively determined and measured. Am. J. Psychology 15, 201–293.
55. Manley, G.T., and Maas, A.I. (2013). Traumatic brain injury: an international knowledge-based approach. JAMA 310, 473–474.
56. Ferguson, A.R., Nielson, J.L., Cragin, M.H., Bandrowski, A.E., and Martone, M.E. (2014). Big data from small data: data-sharing in the 'long tail' of neuroscience. Nat. Neurosci. 17, 1442–1447.
57. Nielson, J.L., Paquette, J., Kloke, J., Liu, A.W., Guandique, C.F., Inoue, T., Irvine, K.A., Gensel, J.C., Petrossian, T.C., Lum, P.Y., Carlsson, G.E., Manley, G.T., Beattie, M.S., Bresnahan, J.C., Ferguson, A.R. (2015). Topological data analysis for discovery in preclinical spinal cord injury and traumatic brain injury. Nature communications In press.
58. Friedli, L., Rosenzweig, E.S., Barraud, Q., Schubert, M., Dominici, N., Awai, L., Nielson, J.L., Musienko, P., Nout-Lomas, Y., Zhong, H., Zudnowski, S., Roy, R.R., Strand, S.C., van den Brand, R., Havton, L.A., Beattie, M.S., Bresnahan, JC., Bezard, E., Bloch, J., Edgerton, V.R.,, Ferguson A.R., Curt, A., Tuszynski, M.H., and Courtine, G. (2015). Pronounced species divergence in corticospinal tract reorganization and functional recovery after lateralized spinal cord injury favors primates. Sci. Transl. Med. 7, 302ra134.
59. Awai, L., Bollinger, M., Ferguson, A.R., Courtine, G., and Curt, A. (2015). Influence of spinal cord integrity on gait control in human spinal cord injury. Neurorehabil. Neural Repair. Epub ahead of print.

Address correspondence to:
Jason F. Talbott, MD, PhD
Department of Radiology
San Francisco General Hospital
1001 Potrero Avenue, Room 1X57C
San Francisco, CA 94110
or
Adam R. Ferguson, PhD
Neurological Surgery, Box 0899
UCSF Brain and Spinal Injury Center
1001 Potrero Avenue, Building 1, Room 101
San Francisco, CA 94143

E-mail: Jason.talbott@ucsf.edu;
adam.ferguson@ucsf.edu